Journal Pre-proofs

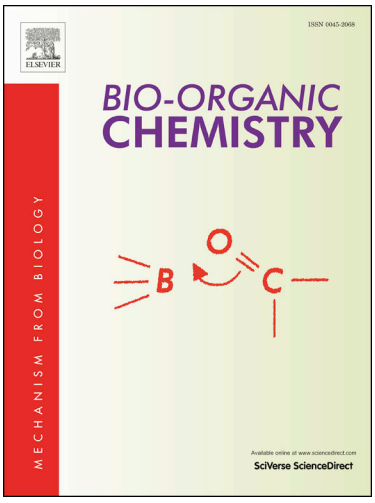

Design and synthesis of novel pyridazine *N*-aryl acetamides: *In-vitro* evaluation of α-glucosidase inhibition, docking, and kinetic studies

Setareh Moghimi, Mahsa Toolabi, Somayeh Salarinejad, Loghman Firoozpour, Seyed Esmaeil Sadat Ebrahimi, Fatemeh Safari, Somayeh Mojtabavi, Mohammad Ali Faramarzi, Alireza Foroumadi

PII: S0045-2068(20)31368-7
DOI: https://doi.org/10.1016/j.bioorg.2020.104071
Reference: YBIOO 104071

To appear in: *Bioorganic Chemistry*

Received Date: 21 April 2020
Revised Date: 21 June 2020
Accepted Date: 2 July 2020

Please cite this article as: S. Moghimi, M. Toolabi, S. Salarinejad, L. Firoozpour, S. Esmaeil Sadat Ebrahimi, F. Safari, S. Mojtabavi, M. Ali Faramarzi, A. Foroumadi, Design and synthesis of novel pyridazine *N*-aryl acetamides: *In-vitro* evaluation of α-glucosidase inhibition, docking, and kinetic studies, *Bioorganic Chemistry* (2020), doi: https://doi.org/10.1016/j.bioorg.2020.104071

Design and synthesis of novel pyridazine *N*-aryl acetamides: *In-vitro* evaluation of α-glucosidase inhibition, docking, and kinetic studies

Setareh Moghimi [a], Mahsa Toolabi [b], Somayeh Salarinejad [c], Loghman Firoozpour [a], Seyed Esmaeil Sadat Ebrahimi [c], Fatemeh Safari [d], Somayeh Mojtabavi,[e] Mohammad Ali Faramarzi [e], Alireza Foroumadi [a, c, **]

[a] *Drug Design and Development Research Center, The Institute of Pharmaceutical Sciences (TIPS), Tehran University of Medical Sciences, Tehran, Iran*

[b]*Department of Medicinal Chemistry, School of Pharmacy, Ahvaz Jundishapur University of Medical Sciences, Ahvaz, Iran*

[c] *Department of Medicinal Chemistry, Faculty of Pharmacy, Tehran University of Medical Sciences, Tehran, Iran*

[d] *Department of Biology, Faculty of Science, University of Guilan, Rasht, Iran*

[e] *Department of Pharmaceutical Biotechnology, Faculty of Pharmacy, Tehran University of Medical Sciences, Tehran, Iran*

Acknowledgement

This work was supported and funded by a grant from Iran National Science Foundation (INSF); grant no. 96011863.

Conflict of Interest

The authors declare no conflict of interest.

Corresponding author:

** E-mail: aforoumadi@yahoo.com (A. Foroumadi); Tel.: 98 21 66406757; Fax: 98 21 66461178.

Abstract

We herein applied the four step-synthetic route to prepare the pyridazine core attached to the various *N*-aryl acetamides. By this approach, a new series of pyridazine-based compounds were synthesized, characterized and evaluated for their activities against α-glucosidase enzyme. *In-vitro* α-glucosidase assay established that twelve compounds are more potent than acarbose. Compound **7a** inhibited α-glucosidase with the IC_{50} value of 70.1 μM. The most potent compounds showed no cytotoxicity against HDF cell line. Molecular docking and kinetic studies were performed to determine the modes of interaction and inhibition, respectively.

.

Keywords: Pyridazine; Glucosidase inhibitor; Lawesson's reagent; Antidiabetic drug

1. Introduction

Diabetes (diabetes mellitus) is a chronic metabolic disease, characterized by the increased blood sugar, resulted from defects in the action or secretion of insulin. The cardiovascular, retinopathy, kidney failure, amputation, eyesight difficulties, and diabetic neuropathy problems are known as the complicated symptoms resulted from diabetes. This health problem is divided to type 1 and type 2 and nearly 90% of all cases of diabetes are type 2. This disease is affecting millions of people globally and the increasing number of patients up to 642 million is expected by 2040 [1,2]. In addition, this disease will become the seventh cause of death by 2030. The public health crisis stemming from long term complications of diabetes, the increasing rate of prevalence among people specifically type 2 (T2DM) and its long term complications urged the pressing need for novel chemotherapies with better safety profiles to combat diabetes [3]. The efforts in the discovery of novel agents should be accompanied by exercise and dietary modifications. The antidiabetic agents currently used to control blood glucose level are sulfonyl ureas, thiazolidinediones [4], biguanides [5], dipeptidyl peptidase-4 (DPP-4) inhibitors [6], GLP-1 agonists [7], and SGLT2 inhibitors [8-11]. The glycemic control in type 2 diabetes is also achieved by α-glucosidase inhibitors [12,13] involving acarbose, miglitol, and vaglibose, used as monotherapy or in combination with insulin or other oral drugs. The function of this class of inhibitors led to the reduced postprandial hyperglycemia by retarding the digestion of carbohydrates and release of glucose. Despite the therapeutic benefits associated with currently available drugs, the side effects including decreased carbohydrate digestion, increased hyperglycemia risk, obesity and possible cancer risk limited their uses and highlighted the ongoing needs to survey for new drug candidates.

Pyridazines and their oxo-derivatives are known as the privileged heteroaromatic skeleton due to the important bioactivities associated with these compounds involving antihypertensive, antifungal, anti-inflammatory, anticancer, and antimicrobial activities [14-19]. Regarding this fact, there has been extensive attention toward the synthesis of novel compounds containing pyridazine moiety and evaluation their bioactivities. Moreover, amide bond is ubiquitously present in drug molecules and biologically active compounds because of its unique features including the polarity, amide proton exchange rate, and protein binding. For instance, this functional group is found in lidocaine, mepivacaine, prilocaine, ceramide drugs used as anesthetics [20].

Bioisosterism is a fundamental concept for medicinal chemists to rationally modify and optimize the compounds to design more potent drug candidates [21,22]. Regarding the previous reports on the α-glucosidase inhibitory activity of triazine-containing compounds [23-27], we have chosen pyridazine ring as triazine bioisoster to study their glucosidase inhibitory activity. The purpose of the current work is to synthesize a series of pyridazine-*N*-aryl acetamide hybrid system and evaluate them as α-glucosidase inhibitors, so, in continuation of our work focused on the synthesis and biological evaluation of novel heterocyclic compounds [28-31], herein, our results are presented.

Some compounds with α-glucosidase inhibitory activity are depicted in Figure 1.

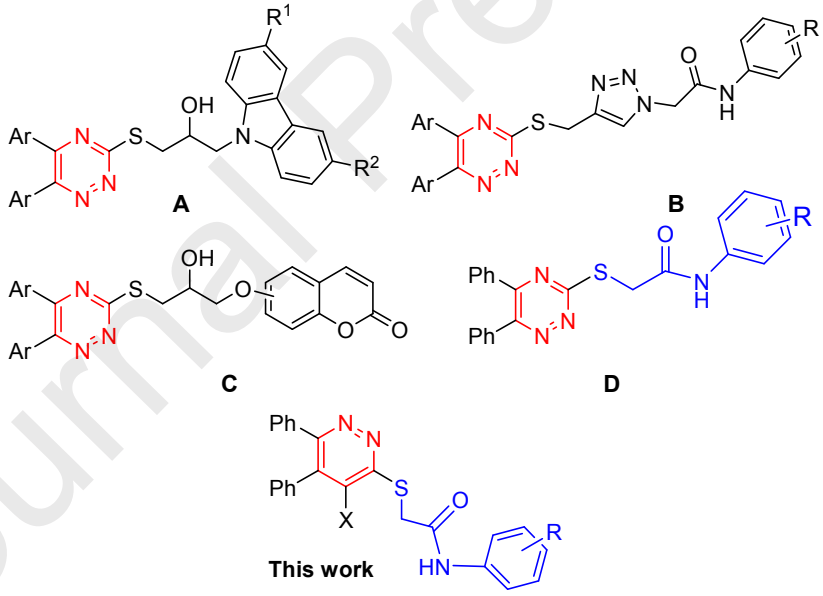

Figure 1. Some reported α-glucosidase inhibitors containing the triazine skeleton.

2. Experimental

2.1 General chemistry

All commercially available reagents and solvents, used without further purification, were purchased from Merck and Sigma-Aldrich companies. Bruker FT-500 MHz spectrometer was used to confirm the structure of the target compounds by ^{1}H- and ^{13}C-NMR spectra in

DMSO-d_6 as the solvent. Chemical shifts reported in δ parts per million (ppm) downfield from tetramethylsilane (TMS) as the internal standard. All reactions were monitored through thin-layer chromatography (TLC) on silica gel 250 mm, F254 plastic sheets. Elemental analysis was recorded by a Perkin Elmer 2400 (automatic elemental analyzer). Melting points were determined with a Kofler hot-plate microscope apparatus and are uncorrected. IR spectroscopy was performed using a Nicolet FT-IR Magna 550 spectrograph (KBr disks).

2.1.1. General procedure for the synthesis of 2-hydrazono-1,2-diphenylethanone (2)

To the warm solution of benzil (10 mmol) in methanol (50 ml), hydrazine hydrate (12 mmol) was added dropwise. The reaction was stirred at reflux temperature for 10 minutes. Upon cooling, the precipitate was filtered and washed with cold methanol [32].

2.1.2 General procedure for the synthesis of ethyl-2,3-dihydro-3-oxo-5,6-diphenylpyridazine-4-carboxylate (3)

To the chilled solution of absolute ethanol (200 mL), sodium (0.05 mol) was carefully added. After obtaining sodium ethoxide solution, 0.05 mol of 2-hydrazono-1,2-diphenyl ethanone was added followed by the addition of diethyl malonate (0.075 mol). Then, the reaction was refluxed for 3 h. After this time, the mixture was concentrated under vaccum and acidifed by HCl (1M). The desired product was collected and washed with water [33].

2.1.3. General procedure for the synthesis ethyl-3-mercapto-5,6-diphenylpyridazie-4-carboxylate (4)

To the solution of compound **3** (20 mmol) in toluene (150 mL) was added Lawesson's reagent (10 mmol) and the mixture was allowed to reflux for 18 h. The reaction was then concentrated and the residue was purified by crystallization from petroleum ether/ethyl acetate [34].

2.1.4. General procedure for the synthesis of *N*-aryl acetamide (6)

To the chilled solution of the appropriate amine (10 mmol) and triethyl amine (10 mmol), chloroacetyl chloride (10 mmol) was added dropwise. The reaction was continued at room temperature upon completion, checked by TLC. Then, petroleum ether was added to the mixture and the resultant solid was filtered, washed and used without further purification.

2.1.5. General procedure for the synthesis of compounds (7a-i)

The mixture of compound **4** (1 mmol) and K_2CO_3 (1 mmol) in DMF (10 mL) was stirred for 10 min. at room temperature. Then, *N*-aryl acetamides (1 mmol) and catalytic amounts of KI were added to the mixture and the reaction was continued at 50 ^oC. Upon completion, checked by TLC, the ice/water solution was added to the mixture. The precipitate was filtered and recrystallized from petroleum ether/ethyl acetate. If no solid obtained, the mixture would be extracted with ethyl acetate and the residue was purified by column chromathography (different ratios of petroleum ether/ethyl acetate).

2.1.5.1. Ethyl 3-((2-oxo-2-(phenylamino)ethyl)thio)-5,6-diphenylpyridazine-4-carboxylate (7a)

White solid; yield: 80%; mp: 109-111 °C; IR (KBr, cm^{-1}): 3354 (N-H), 1724 (C=O), 1690 (C=O), 1319, 1194; ^{1}H NMR (500 MHz, DMSO-d_6) δ: 0.90 (t, J = 7.1 Hz, 3H), 4.09 (q, J = 7.2 Hz, 2H), 4.42 (s, 2H), 7.06 (t, J = 7.5 Hz, 1H), 7.15 (d, J = 6.8 Hz, 2H), 7.25-7.35 (m, 10H), 7.61 (d, J = 8.1 Hz, 2H), 10.41 (s, 1H); ^{13}C NMR (125 MHz, DMSO-d_6) δ: 13.2, 34.7, 59.2, 111.2, 123.3 (2C), 124.2, 126.3 (2C), 126.4 (2C), 126.7, 127.1 (2C), 127.3 (2C), 127.4, 127.8 (2C), 131.2, 137.3, 137.4, 146.5, 149.0, 164.5, 168.3; Anal. Calcd. For $C_{27}H_{23}N_3O_3S$: C, 69.06; H, 4.94; N, 8.95. Found: C, 69.28; H, 4.61; N, 8.71; ESI-MS *m/z*: calculated: 469.1 $[M]^+$; obtained: 470.2 $[M+H]^+$.

2.1.5.2. Ethyl 3-((2-oxo-2-(p-tolylamino)ethyl)thio)-5,6-diphenylpyridazine-4-carboxylate (7b)

Off-white solid; yield: 80%; mp: 160-162 °C; IR (KBr, cm^{-1}): 3317 (N-H), 1728 (C=O), 1674 (C=O), 1298, 1201; ^{1}H NMR (500 MHz, DMSO-d_6) δ: 0.90 (t, J = 7.1 Hz, 3H), 2.25 (s, 3H), 4.08 (q, J = 7.2 Hz, 2H), 4.40 (s, 2H), 7.11-7.15 (m, 4H), 7.26-7.36 (m, 8H), 7.49 (d, J = 7.9 Hz, 2H), 10.33 (s, 1H); ^{13}C NMR (125 MHz, DMSO-d_6) δ: 12.8, 19.8, 34.5, 61.5, 118.5 (2C), 127.3 (2C), 127.7 (2C), 128.0, 128.2, 128.4 (2C), 128.6 (2C), 129.0 (2C), 129.6, 131.7, 133.1, 134.6, 135.4, 135.9, 155.1, 156.8, 163.5, 164.8; Anal. Calcd. For $C_{28}H_{25}N_3O_3S$: C, 69.54; H, 5.21; N, 8.69. Found: C, 69.75; H, 5.49; N, 8.81; ESI-MS *m/z*: calculated: 483.1 $[M]^+$; obtained: 484 .2 $[M+H]^+$.

2.1.5.3. Ethyl 3-((2-((4-isopropylphenyl)amino)-2-oxoethyl)thio)-5,6-diphenylpyridazine-4-carboxylate (7c)

Off-white solid; yield: 75%; mp: 164-166 °C; IR (KBr, cm^{-1}): 3347 (N-H), 1730 (C=O), 1669 (C=O), 1325, 1188; ^{1}H NMR (500 MHz, DMSO-d_6) δ: 0.90 (t, J = 7.1 Hz, 3H), 1.17 (d, J = 6.8 Hz, 6H), 2.80-2.86 (m, 1H), 4.09 (q, J = 7.1 Hz, 2H), 4.41 (s, 2H), 7.15 (d, J = 7.1 Hz, 2H), 7.19 (d, J = 8.0 Hz, 2H), 7.24-7.45 (m, 8H), 7.53 (d, J = 8.0 Hz, 2H), 10.36 (s, 1H); ^{13}C NMR (125 MHz, DMSO-d_6) δ: 12.8, 23.3, 32.3, 34.5, 38.9, 61.5, 118.6 (2C), 125.9 (2C), 127.3 (2C), 127.7 (2C), 128.0, 128.2, 128.4 (2C), 129.0 (2C), 129.6, 133.1, 134.6, 135.4, 136.2, 142.9, 155.1, 156.8, 163.5, 164.8; Anal. Calcd. For $C_{30}H_{29}N_3O_3S$: C, 70.43; H, 5.71; N, 8.21. Found: C, 70.12; H, 5.47; N, 8.54; ESI-MS *m/z*: calculated: 511.2 $[M]^+$; obtained: 512.3 $[M+H]^+$.

2.1.5.4. Ethyl 3-((2-((3-ethynylphenyl)amino)-2-oxoethyl)thio)-5,6-diphenylpyridazine-4-carboxylate (7d)

Off-white solid; yield: 70%; mp: 83-85 °C; IR (KBr, cm^{-1}): 3288 (N-H), 1727 (C=O), 1688 (C=O), 1326, 1195; ^{1}H NMR (500 MHz, DMSO-d_6) δ: 0.89 (t, J = 7.1 Hz, 3H), 4.09 (q, J = 7.1 Hz, 2H), 4.19 (s, 1H), 4.43 (s, 2H), 7.14-7.18 (m, 3H), 7.22-7.36 (m, 9H), 7.59 (d, J = 8.3 Hz, 1H), 7.83 (s, 1H), 10.56 (s, 1H); ^{13}C NMR (125 MHz, DMSO-d_6) δ: 12.8, 34.5, 61.6, 80.0, 82.7, 119.1, 121.3, 121.5, 126.0, 127.3 (2C), 127.7 (2C), 128.0, 128.2, 128.4 (2C), 128.7, 129.0 (2C), 129.6, 133.1, 134.6, 135.4, 138.6, 155.0, 156.8, 163.5, 165.4; Anal. Calcd. For

$C_{29}H_{23}N_3O_3S$: C, 70.57; H, 4.70; N, 8.51. Found: C, 70.21; H, 4.59; N, 8.84; ESI-MS *m/z*: calculated: 493.1 $[M]^+$; obtained: 494.1 $[M+H]^+$.

2.1.5.5. Ethyl 3-((2-((4-methoxyphenyl)amino)-2-oxoethyl)thio)-5,6-diphenylpyridazine-4-carboxylate (7e)

Off-white solid; yield: 82%; mp: 142-145 °C; IR (KBr, cm^{-1}): 3312 (N-H), 1722 (C=O), 1672 (C=O), 1300, 1161; ^1H NMR (500 MHz, DMSO-d_6) δ: 0.89 (t, J = 6.6 Hz, 3H), 3.71 (s, 3H), 4.09 (q, J = 7.2 Hz, 2H), 4.39 (s, 2H), 6.89 (d, J = 7.9 Hz, 2H), 7.14 (d, J = 5.9 Hz, 2H), 7.23-7.33 (m, 8H), 7.52 (d, J = 7.9 Hz, 2H), 10.33 (s, 1H); ^{13}C NMR (125 MHz, DMSO-d_6) δ: 13.3, 34.9, 55.1, 62.1, 113.9 (2C), 120.6 (2C), 127.8 (2C), 128.3 (2C), 128.5, 128.8 (2C), 128.9, 129.6 (2C), 130.2, 132.1, 133.6, 135.1, 135.9, 155.2, 155.7, 157.3, 164.1, 165.0; Anal. Calcd. For $C_{28}H_{25}N_3O_4S$: C, 67.32; H, 5.04; N, 8.41; Found: C, 67.59; H, 5.21; N, 8.12; ESI-MS *m/z*: calculated: 499.2 $[M]^+$; obtained: 500.1 $[M+H]^+$.

2.1.5.6. Ethyl 3-((2-((4-fluorophenyl)amino)-2-oxoethyl)thio)-5,6-diphenylpyridazine-4-carboxylate (7f)

Yellow solid; yield: 77%; mp: 159-161 °C; IR (KBr, cm^{-1}): 3342 (N-H), 1721 (C=O), 1679 (C=O), 1309, 1214; ^1H NMR (500 MHz, DMSO-d_6) δ: 0.90 (t, J = 7.2 Hz, 3H). 4.09 (q, J = 7.2 Hz, 2H), 4.41 (s, 2H), 7.14-7.17 (m, 4H), 7.24-7.36 (m, 8H), 7.64 (dd, J = 9.4, 5.1 Hz, 2H), 10.46 (s, 1H); ^{13}C NMR (125 MHz, DMSO-d_6) δ: 12.8, 34.4, 61.5, 114.8 (d, J = 22.0 Hz, 2C), 120.3 (d, J = 7.6 Hz, 2C), 127.3 (2C), 127.7 (2C), 128.0, 128.2, 128.4 (2C), 129.0 (2C), 129.6, 133.1, 134.6, 134.8, 135.4, 155.0, 156.8, 157.5 (d, J = 238.5 Hz), 163.5, 165.0; Anal. Calcd. For $C_{27}H_{22}FN_3O_3S$: C, 66.52; H, 4.55; N, 8.62; Found: C, 66.75; H, 4.29; N, 8.81; ESI-MS *m/z*: calculated: 487.1 $[M]^+$; obtained: 488.2 $[M+H]^+$.

2.1.5.7. Ethyl 3-((2-((4-chlorophenyl)amino)-2-oxoethyl)thio)-5,6-diphenylpyridazine-4-carboxylate (7g)

Yellow solid; yield: 75%; mp: 149-151 °C; IR (KBr, cm^{-1}): 3331 (N-H), 1724 (C=O), 1683 (C=O), 1324, 1166; ^1H NMR (500 MHz, DMSO-d_6) δ: 0.90 (t, J = 7.2 Hz, 3H), 4.09 (q, J = 7.1 Hz, 2H), 4.42 (s, 2H), 7.15 (d, J = 7.1 Hz, 2H), 7.23-7.27 (m, 5H), 7.31-7.41 (m, 5H), 7.65 (d, J = 8.5 Hz, 2H), 10.56 (s, 1H); ^{13}C NMR (125 MHz, DMSO-d_6) δ: 12.8, 34.5, 61.6, 120.0 (2C), 126.4, 127.3 (2C), 127.7 (2C), 128.0, 128.1 (2C), 128.2, 128.4 (2C), 129.0 (2C), 129.6, 133.1, 134.6, 135.4, 137.4, 155.0, 156.8, 163.5, 165.3; Anal. Calcd. For $C_{27}H_{22}ClN_3O_3S$: C, 64.34; H, 4.40; N, 8.34. Found: C, C, 64.15; H, 4.61; N, 8.54; ESI-MS *m/z*: calculated: 503.1 $[M]^+$; obtained: 504.1 $[M+H]^+$.

2.1.5.8. Ethyl 3-((2-((3,5-dichlorophenyl)amino)-2-oxoethyl)thio)-5,6-diphenylpyridazine-4-carboxylate (7h)

Off-white solid; yield: 74%; mp: 133-135°C; IR (KBr, cm^{-1}): 3412 (N-H), 1721 (C=O), 1664 (C=O), 1300, 1187; ^1H NMR (500 MHz, DMSO-d_6) δ: 0.89 (t, J = 7.7 Hz, 3H), 4.09 (q, J = 7.6 Hz, 2H), 4.45 (s, 2H), 7.14 (d, J = 7.1 Hz, 2H), 7.24-7.34 (m, 9H), 7.70 (s, 2H), 10.80 (s, 1H); ^{13}C NMR (125 MHz, DMSO-d_6) δ: 12.7, 34.6, 61.6, 116.6 (2C), 122.0, 127.3 (2C), 127.7 (2C), 128.0, 128.2, 128.4 (2C), 129.0 (2C), 129.6, 133.1, 133.6 (2C), 134.7, 135.3, 140.7,

154.9, 156.8, 163.5, 165.9; Anal. Calcd. For $C_{27}H_{21}Cl_2N_3O_3S$: C, 60.23; H, 3.93; N, 7.80. Found: C, 60.51; H, 3.67; N, 7.71; ESI-MS *m/z*: calculated: 537.1 $[M]^+$; obtained: 538.3 $[M+H]^+$.

2.1.5.9. Ethyl 3-((2-((4-cyanophenyl)amino)-2-oxoethyl)thio)-5,6-diphenylpyridazine-4-carboxylate (7i)

Yellow solid; yield: 71%; mp: 194-196 °C; IR (KBr, cm^{-1}): 3291 (N-H), 2216 (C≡N), 1724 (C=O), 1671 (C=O), 1324, 1199; ^1H NMR (500 MHz, DMSO-d_6) δ: 0.91 (t, J = 7.0 Hz, 3H), 4.06-4.13 (q, J = 7.1 Hz, 2H), 4.46 (s, 2H), 7.15 (d, J = 7.0 Hz, 2H), 7.25-7.33 (m, 8H), 7.77-7.82 (m, 4H), 10.87 (s, 1H); ^{13}C NMR (125 MHz, DMSO-d_6) δ: 12.7, 34.6, 61.6, 104.6, 118.4, 118.5 (2C), 127.3 (2C), 127.7 (2C), 128.0, 128.2, 128.4 (2C), 129.0 (2C), 129.5, 132.8 (2C), 133.1, 134.7, 135.3, 142.6, 154.9, 156.9, 163.5, 166.0; Anal. Calcd. For $C_{28}H_{22}N_4O_3S$: C, 68.00; H, 4.48; N, 11.33. Found: C, 68.24; H, 4.19; N, 11.58; ESI-MS *m/z*: calculated: 494.1 $[M]^+$; obtained: 495.4 $[M+H]^+$.

2.1.6. General procedure for the preparation of compounds 8a-8e

The appropriate compounds (1 mmol) were dissolved in ethanol (5 mL) and after that NaOH solution (1M, 5 mL) was added and the mixture was refluxed. Upon completion, checked by TLC, the mixture was acidified to pH = 1 and the resultant solid was filtered and washed with water.

2.1.6.1. 3-((2-Oxo-2-(phenylamino)ethyl)thio)-5,6-diphenylpyridazine-4-carboxylic acid (8a)

Off-white solid; yield: 82%; mp: 122-124 °C; IR (KBr, cm^{-1}): 3376 (N-H), 3056 (COOH), 1719 (C=O), 1660 (C=O), 1326, 1200; ^1H NMR (500 MHz, DMSO-d_6) δ: 4.45 (s, 2H), 7.16-7.20 (m, 2H), 7.23-7.36 (m, 9H), 7.79-7.83 (m, 4H), 10.88 (s, 1H), 12.25 (brs, 1H). ^{13}C NMR (125 MHz, DMSO-d_6) δ: 35.8, 115.3, 121.2 (2C), 125.3, 127.4 (2C), 127.9, 128.1 (2C), 128.1 (2C), 128.3 (2C), 128.5, 129.0 (2C), 132.4, 133.3, 136.2, 138.6, 147.6, 148.9, 166.9, 169.5; Anal. Calcd. For $C_{25}H_{19}N_3O_3S$: C, 68.01; H, 4.34; N, 9.52. Found: C, 68.32; H, 4.15; N, 9.84. ESI-MS *m/z*: calculated: 441.1 $[M]^+$; obtained: 442.4 $[M+H]^+$.

2.1.6.2. 3-((2-((3-Ethynylphenyl)amino)-2-oxoethyl)thio)-5,6-diphenylpyridazine-4-carboxylic acid (8b)

Off-white solid; yield: 78%; mp: 201-203 °C; IR (KBr, cm^{-1}): 3308 (N-H), 3105 (COOH), 1695 (C=O), 1681 (C=O), 1309, 1217; ^1H NMR (500 MHz, DMSO-d_6) δ: 4.19 (s, 1H), 4.41 (s, 2H), 7.17-7.19 (m, 3H), 7.25-7.37 (m, 9H), 7.60 (d, J = 8.4 Hz, 1H), 7.83 (s, 1H), 10.54 (s, 1H), 12.14 (brs, 1H); ^{13}C NMR (125 MHz, DMSO-d_6) δ: 35.1, 77.5, 79.3, 122.4, 122.6, 123.9, 126.5 (2C), 128.5, 128.6, 129.0, 129.3, 129.6 (2C), 130.3, 130.4 (2C), 130.5 (2C), 135.2, 136.6, 138.6, 138.8, 158.0, 159.2, 167.8, 168.1; Anal. Calcd. For $C_{27}H_{19}N_3O_3S$: C, 69.66; H, 4.11; N, 9.03. Found: C, 69.45; H, 4.31; N, 9.37; ESI-MS *m/z*: calculated: 465.1 $[M]^+$; obtained: 466.2 $[M+H]^+$.

2.1.6.3. 3-((2-((4-Chlorophenyl)amino)-2-oxoethyl)thio)-5,6-diphenylpyridazine-4-carboxylic acid (8c)

Off-white solid; yield: 80%; mp: 169-171 °C; IR (KBr, cm^{-1}): 3425 (N-H), 3081 (COOH), 1691 (C=O), 1683 (C=O), 1321, 1200; ^{1}H NMR (500 MHz, DMSO-d_6) δ: 4.41 (s, 2H), 7.18 (d, J = 8.1 Hz, 2H), 7.26-7.34 (m, 8H), 7.39 (d, J = 8.5 Hz, 2H), 7.66 (d, J = 8.6 Hz, 2H), 10.57 (s, 1H), 12.17 (brs, 1H); ^{13}C NMR (125 MHz, DMSO-d_6) δ: 34.7, 124.4 (2C), 128.6, 128.8 (2C), 129.9 (2C), 130.1 (2C), 130.4, 130.6 (2C), 131.1 (2C), 132.4, 134.4, 135.0, 136.3, 140.6, 141.7, 154.9, 161.9, 168.8, 169.6; Anal. Calcd. For $C_{25}H_{18}ClN_3O_3S$: C, 63.09; H, 3.81; N, 8.83. Found: C, 63.27; H, 3.52; N, 8.99; ESI-MS *m/z*: calculated: 475.1 $[M]^+$; obtained: 476.1 $[M+H]^+$.

2.1.6.4. 3-((2-((3,5-Dichlorophenyl)amino)-2-oxoethyl)thio)-5,6-diphenylpyridazine-4-carboxylic acid (8d)

Off-white solid; yield: 79%; mp: 161-163 °C; IR (KBr, cm^{-1}): 3485 (N-H), 3244 (COOH), 1687 (C=O), 1677 (C=O), 1326, 1203; ^{1}H NMR (500 MHz, DMSO-d_6) δ: 4.42 (s, 2H), 7.16-7.20 (m, 2H), 7.25-7.34 (m, 9H), 7.70 (d, J = 1.9 Hz, 2H), 10.79 (s, 1H), 12.24 (brs, 1H); ^{13}C NMR (125 MHz, DMSO-d_6) δ: 33.2, 118.0 (2C), 122.4, 128.4 (2C), 128.6 (2C), 128.9, 129.1 (2C), 129.6 (2C), 130.3, 132.9, 133.5, 134.8, 134.9 (2C), 140.0, 140.2, 153.4, 160.4, 167.3, 168.1; Anal. Calcd. For $C_{25}H_{17}Cl_2N_3O_3S$: C, 58.83; H, 3.36; N, 8.23. Found: C, 58.98; H, 3.51; N, 8.01. ESI-MS *m/z*: calculated: 475.1 $[M]^+$; obtained:510.4 $[M+H]^+$.

2.1.6.5. 3-((2-((4-cyanophenyl)amino)-2-oxoethyl)thio)-5,6-diphenylpyridazine-4-carboxylic acid (8e)

Off-white solid; yield: 75%; mp: 182-184 °C; IR (KBr, cm^{-1}): 3395 (N-H), 3051 (COOH), 2221 (C$\equiv$N), 1705 (C=O), 1671 (C=O), 1301, 1166; ^{1}H NMR (500 MHz, DMSO-d_6) δ: 4.43 (s, 2H), 7.07 (t, J = 7.4 Hz, 1H), 7.17-7.21 (m, 2H), 7.25-7.34 (m, 9H), 7.64 (d, J = 8.0 Hz, 2H), 10.44 (s, 1H), 12.33 (s, 1H); ^{13}C NMR (125 MHz; DMSO-d_6) δ: 33.2, 108.7, 118.5, 120.1 (2C), 128.6 (2C), 128.9, 129.1 (2C), 129.6 (2C), 130.9, 132.0 (2C), 132.9 (2C), 133.5, 134.8, 140.2, 141.2, 153.4, 160.4, 167.3, 168.1; Anal. Calcd. For $C_{26}H_{18}N_4O_3S$: C, 66.94; H, 3.89; N, 12.01. Found: C, 66.71; H, 3.62; N, 12.37; ESI-MS *m/z*: calculated: 466.1 $[M]^+$; obtained: 467.4 $[M+H]^+$.

2.2. Biological Results

2.2.1. *In-vitro* α-glucosidase inhibition assay

α-Glucosidase (Saccharomyces cerevisiae, EC3.2.1.20, 20 U/mg) and substrate (p-nitrophenyl glucopyranoside) were purchased from Sigma-Aldrich. Desired concentrations of enzyme were prepared by potassium phosphate buffer (pH 6.8, 50 mM), and the target

compounds were dissolved in DMSO (10% final concentration). The enzyme solution (20 µL), different concentrations of compounds (20 µL), and potassium phosphate buffer (135 µL) were added to the 96-well plate and incubated at 37 °C for 10 min. Then, *p*-nitrophenyl glucopyranoside as substrate (25 µL, 4 mM) was added to each well and allowed to be incubated at 37 °C for 20 min. Finally, the change in the absorbance was measured at 405 nm by using spectrophotometer (Gen5, Power wave xs2, BioTek, America). DMSO and acarbose were used as the control and standard inhibitor, respectively. The percentage of inhibition for target compounds, control, and the standard inhibitor was calculated by using the following formula:

%Inhibition = [(Abs control Abs sample)/Abs control] × 100

IC_{50} values of tested compounds were obtained from the nonlinear regression curve using the Logit method.

2.2.2. Kinetic studies

The mode of inhibition of the most active compound **7a**, identified with the lowest IC_{50}, was investigated against α-glucosidase activity with different concentrations of p-nitrophenyl α-D-glucopyranoside (2–10 mM) as substrate in the absence and presence of sample **7a** at different concentrations (0, 30, 50, and 70 µM). A Lineweaver–Burk plot was generated to identify the type of inhibition and the Michaelis–Menten constant (K_m) value was determined from plot between reciprocal of the substrate concentration (1/[S]) and reciprocal of enzyme rate (1/V) over various inhibitor concentrations. Experi (K_i) value was constructed by secondary plots of the inhibitor concentration [I] versus Km.

2.2.3. Cytotoxic studies

The cytotoxic studies of selected compounds were performed according to the previously reported literature [28].

2.2.4. Docking studies

Molecular docking study of compound **7a** and **8a** were conducted using Autodock 4.2.1. The crystal structure of *S. cerevisiae isomaltase* (PDB: 3A4A) with 1.6 Å resolution was downloaded from the RCSB data bank. The docking procedure was performed as previously reported. The detailed docking analysis including the 3D and 2D diagram interactions were depicted by Discovery Studio visualizer 4.5 [35].

3. Results and discussion

3.1 Chemistry

The overall synthetic approach is shown in scheme 1. At first, benzil, dissolved in methanol, was treated with hydrazine hydrate to generate compound **2**. Then, the isolated white solid was added to the sodium ethanolate solution, prepared *in situ*, followed by the addition

of diethyl malonate. After stirring at reflux temperature for 3 hours and acidification of the residue, the desired pyridazine **3** was obtained by a tandem one-pot cyclization. Finally, ethyl-3-mercapto-5,6-diphenylpyridazie-4-carboxylate was obtained by the reaction of ethyl-2,3-dihydro-3-oxo-5,6-diphenylpyridazine-4-carboxylate with Lawesson's reagent in toluene at reflux temperature. The procedure for the synthesis of *N*-aryl acetamides was carried out by using the appropriate amines and chloroacetyl chloride using triethyl amine. Compound **5** with different substituents e.g. electron-donating and electron withdrawing at different positions on the phenyl ring could react and provide the corresponding *N*-chloro acetamide derivatives in satisfactory yields. This procedure, called route B and presented in Scheme 1. As schematically presented in route C, the nucleophilic substitution reaction between compounds **4** and **6** in dimethyl formamide (DMF), K_2CO_3, and catalytic amounts of KI afforded final compounds **7a-i** in good yields. The acid analogues of final compounds **8a-e** were obtained by the basic hydrolysis of compounds **7a-i** in ethanol. Our tries to perform the reaction between acid analogue of compound **4** and *N*-phenyl acetamide led to the product in much lower yields.

A series of substituents including methyl, methoxy, ethynyl, isopropyl, fluoro, chloro, and cyano were examined to explore the substrate scope of the reaction and the results are presented in table 1.

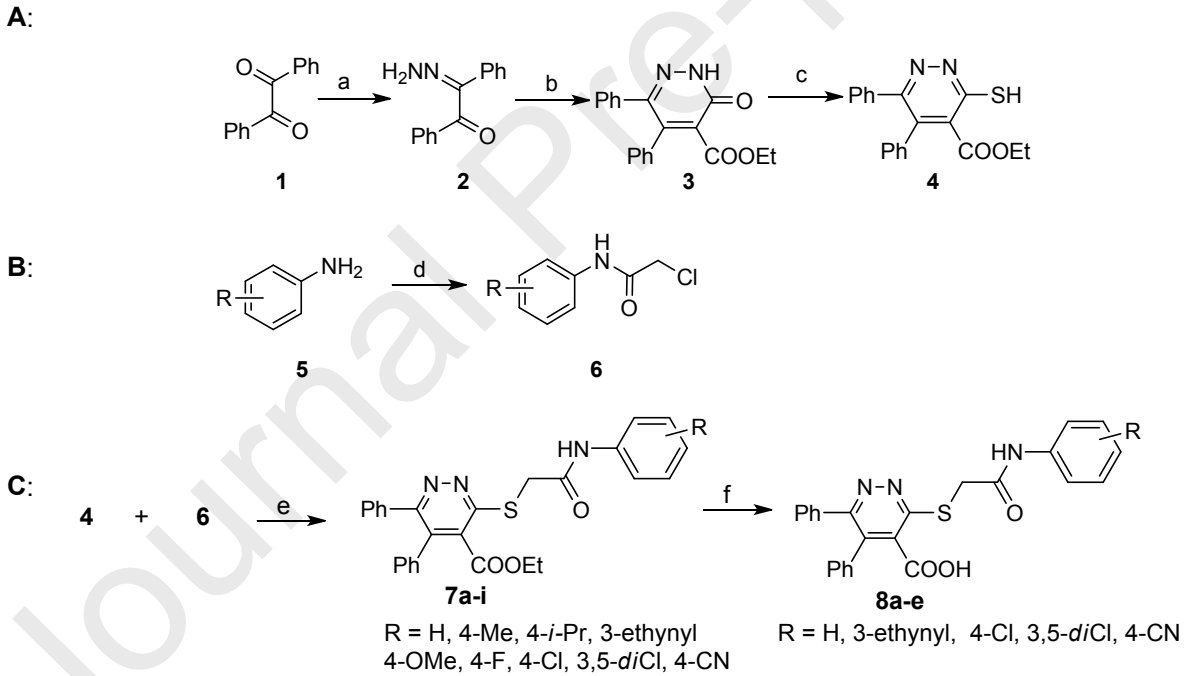

Scheme 1. Synthesis of target compounds. Reagents and conditions: a) hydrazine hydrate, methanol, reflux; b) Na, EtOH, diethyl malonate, reflux; c) Lawesson's reagent, toluene, reflux; d) chloroacetyl chloride, Et_3N, CH_2Cl_2; e) K_2CO_3, KI, *N*-aryl acetamides, DMF, 50 ^oC; f) NaOH (1M), EtOH, reflux.

3.2. α-Glucosidase inhibitory activity

The activity of two series of final compounds (**7a-i**) and (**8a-e**) were investigated and the results were depicted in Table 1. All the ester-containing derivatives showed higher inhibitory activities with IC_{50} values of 70.1-321.6 µM than the activity of acarbose. The most potent compound in this series was the unsubstituted derivative **7a** with IC_{50} value of 70.1 µM which is 10 folds more active than positive control, acarbose, with IC_{50} value of 750 µM.

Then, various hydrophobic substituents including methyl, isopropyl, methoxy, ethynyl, and chlorine were examined at 3- and 4-position of phenyl ring. The introduction of a methyl group at the *para* position of phenyl ring led to the decreased activity against α-glucosidase enzyme with IC_{50} = 161.0 µM. Further enlargement of the methyl group at *para* position, isopropyl, retained the inhibitory activity (**7b** vs **7c**). Interestingly, the introduction of a linear ethynyl group at *meta* position produced compound (**7d,** IC_{50} = 91.0 µM) which is 8 times more potent than positive control. Introducing halogen atoms such as fluoro and chloro to the benzene ring at *para* position led to the weakest compounds in this series with IC_{50s} = 321.6, 300.4 µM, respectively. The presence of fluorine, the electronegative atom, led to compound **7f** exhibiting decreased activity in comparison with chlorine substituted compound **7g**. While, the presence of two chlorine atom at 3 and 5 positions, **7h**, increased the activity (IC_{50} = 123.3 µM). This addition might be resulted in better interactions of compounds with the active site of enzyme. Then, the introduction of a linear and polar group, nitrile, yielded compound **7i** which demonstrated two-times more potency in relation to *para*-substituted fluoro and chloro-containing compounds.

The conversion of ester to acid led to losses in potency in case of unsubstituted and 3,5-dichloro substituents. The presence of electron withdrawing groups involving chlorine and cyano group at *para* position increased the inhibitory activities compared to unsubstituted derivative **8a**. While, an ethynyl group at meta position resulted in nearly two-fold decrease in activity in relation to **8c** and **8e**. In all cases, the comparison between ester and acid analogues revealed that except 4-chloro derivative (**7g** *vs* **8c**), the inhibitory activity of acid analogues decreased.

Table 1. α-Glucosidase inhibitory activity of the target compounds, presented as IC_{50} (µM). [a]

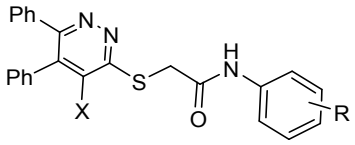

Compound	X	R	IC_{50} (µM)
7a	COOEt	H	70.1 ± 0.6
7b	COOEt	4-Me	161.0 ± 2.1
7c	COOEt	4-*i*Pr	166.8 ± 2.3
7d	COOEt	3-Ethynyl	91.0 ± 1.0

7e	COOEt	4-OMe	154.5 ± 1.9
7f	COOEt	4-F	321.6 ± 4.4
7g	COOEt	4-Cl	300.4 ± 4.1
7h	COOEt	3,5-*di*Cl	123.3 ± 1.4
7i	COOEt	4-CN	140.6 ± 1.7
8a	COOH	H	>750
8b	COOH	3-Ethynyl	457.3 ± 5.3
8c	COOH	4-Cl	278.7 ± 3.6
8d	COOH	3,5-*di*Cl	>750
8e	COOH	4-CN	297.7 ± 3.9
	Acarbose		750.0 ± 10.0

[a]Values are the means of three replicates±standard deviation (SD).

3.3. Kinetic studies

The kinetic studies were utilized to determine the mode of inhibition of the selected target derivatives. The competitive mode of inhibition was determined for the most active compound, **7a**. The unchanged V_{max} value and increased Km value which were determined by Lineweaver-Burk plot indicated that compound **7a** is bound to the active site and competed with the substrate. Moreover, by drawing the plot of the K_m versus different concentrations of inhibitor, an estimate amount of 70 µM was determined for the inhibition constant, K_i.

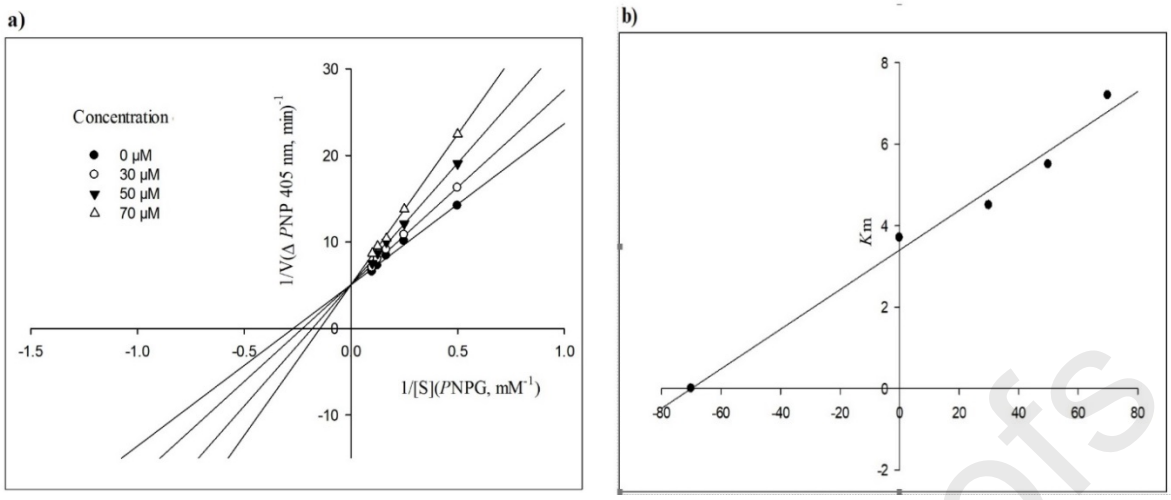

Figure 2. Kinetics of α-glucosidase inhibition by compound **7a**; (a) The Lineweaver-Burk plot in the absence and presence of different concentrations of compound **7a**; (b) The secondary plot between K_m and various concentrations of compound **7a**.

3.4. Cytotoxic studies

The cytotoxic activities of the most active compounds **7a**, **7d**, **8a**, and **8e** were evaluated in relation to normal cell line, Human Dermal Fibroblasts (HDF), using the 3-(4,5-dimethylthiazole-2-yl)2,5-diphenyltetrazolium bromide (MTT) colorimetic assay. According to the obtained IC_{50} values, the results indicated that none of selected compounds were toxic against the normal cell line [28]. The activity of these compounds is similar to etoposide which was used as the positive control

Table 2. *In vitro* antiproliferative effects (IC_{50}, µM) of selected compounds against HDF cell line.[a]

Compound	IC_{50} (µM)
7a	>100
7d	>100
8a	>100
8e	>100
Etoposide	>100

[a]Values were the means of three replicates±standard deviation (SD).

3.5. Docking study

In order to provide insights into the binding interactions of synthesized compounds in the active site of α-glucosidase, molecular docking studies were utilized with the most active compound, **7a** and its acidic analogue, **8a**, using Autodock 4.2.1 package. Since the x-ray crystallographic structure *S. cerevisiae* α-glucosidase isn't accessible, the 3D structure of *S. cerevisiae isomaltase* with PDB ID: 3A4A was downloaded from RCSB web site with 84% similarity to *S. cerevisiae* α-glucosidase. The docking analysis data including the best scoring conformation based on binding energy were illustrated by Discovery Studio visualizer 4.5 and shown in figures 3 and 4.

Figure 3 indicated the interaction of compound **7a** with the active site residues. Compound **7a** interacted with the residues present in the active site of enzyme through several hydrogen bonds and hydrophobic interactions. The amide group established two hydrogen bonds with Glu 277 and Arg 442 and the nitrogen atom of pyridazine also formed another hydrogen bond with Gln 279. Likewise, π-anion and π-π T-shaped interactions formed between phenyl rings and Asp 215, Glu 411, Tyr 72, and Tyr 158, respectively. Two phenyl moieties attached to the pyridazine ring also interacted with Arg 315 via π-alkyl interactions. Furthermore, the formation of π-sulfur interaction between the sulfur atom and the phenyl ring of Phe 303 and some different van der Waals interactions fitted this ligand tightly into the active site of the enzyme.

The interaction of compound **8a** with the active site of enzyme is depicted in figure 4. This compound adopted different binding modes with little resemblance as compared to the compound **7a** (figure 5). In this ligand, formations of hydrogen bonds with Glu 277 and Glu 411 are observed. The phenyl ring adjacent to the amide group and the pyridazine ring formed π-π stacking with Phe 303 and Tyr 158, respectively. Additionally, this compound is involved in hydrophobic interactions with several residues such as Asp 352, Arg 442, Gln 279, and Asp 307.

Generally, compound **7a** formed an additional hydrogen bond and more favorable interactions with the enzyme with higher affinity in comparison to compound **8a**. These interactions along with the optimum binding energy (-9.5 kcal/mol for compound **7a** vs -6.2 kcal/mol for compound **8a**) improved the stability of the ligand-enzyme complex which can be the reason for better inhibitory activity of compound **7a** toward α-glucosidase in biological results.

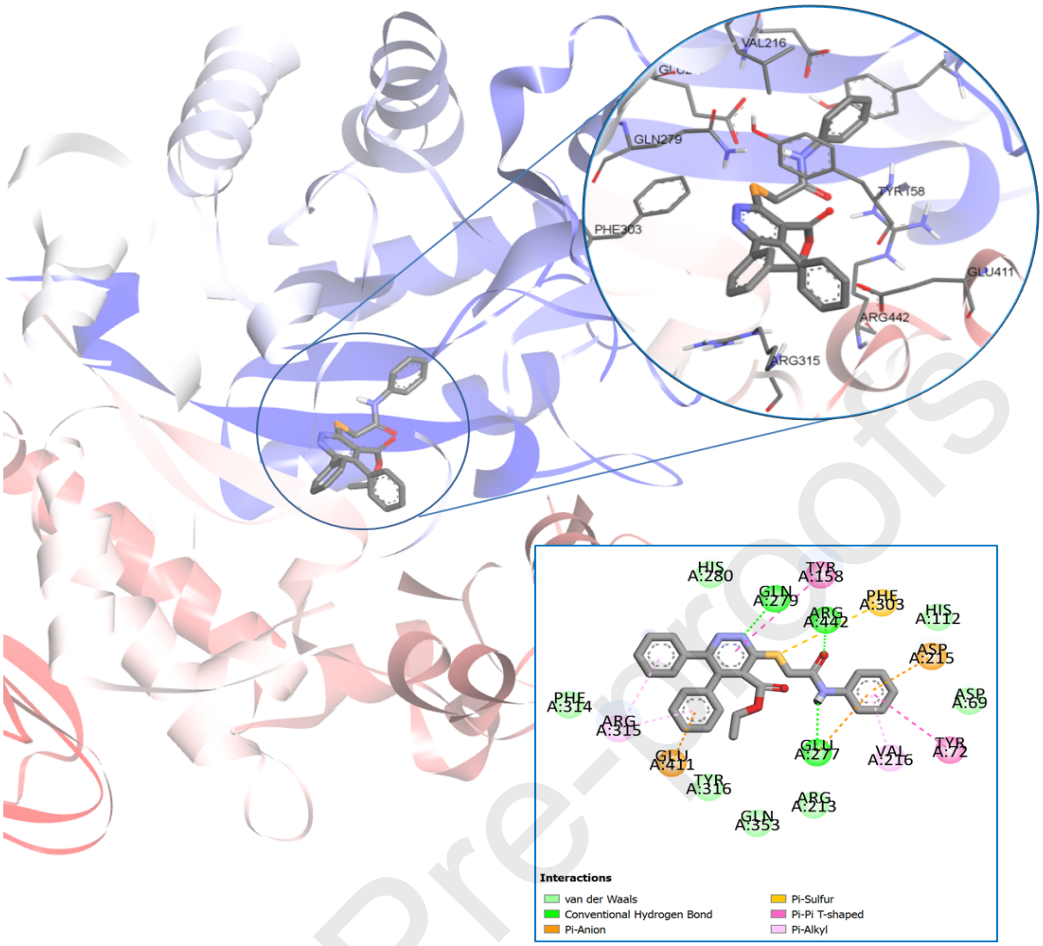

Figure 3. 3D binding conformation and 2D binding conformation of compound **7a**.

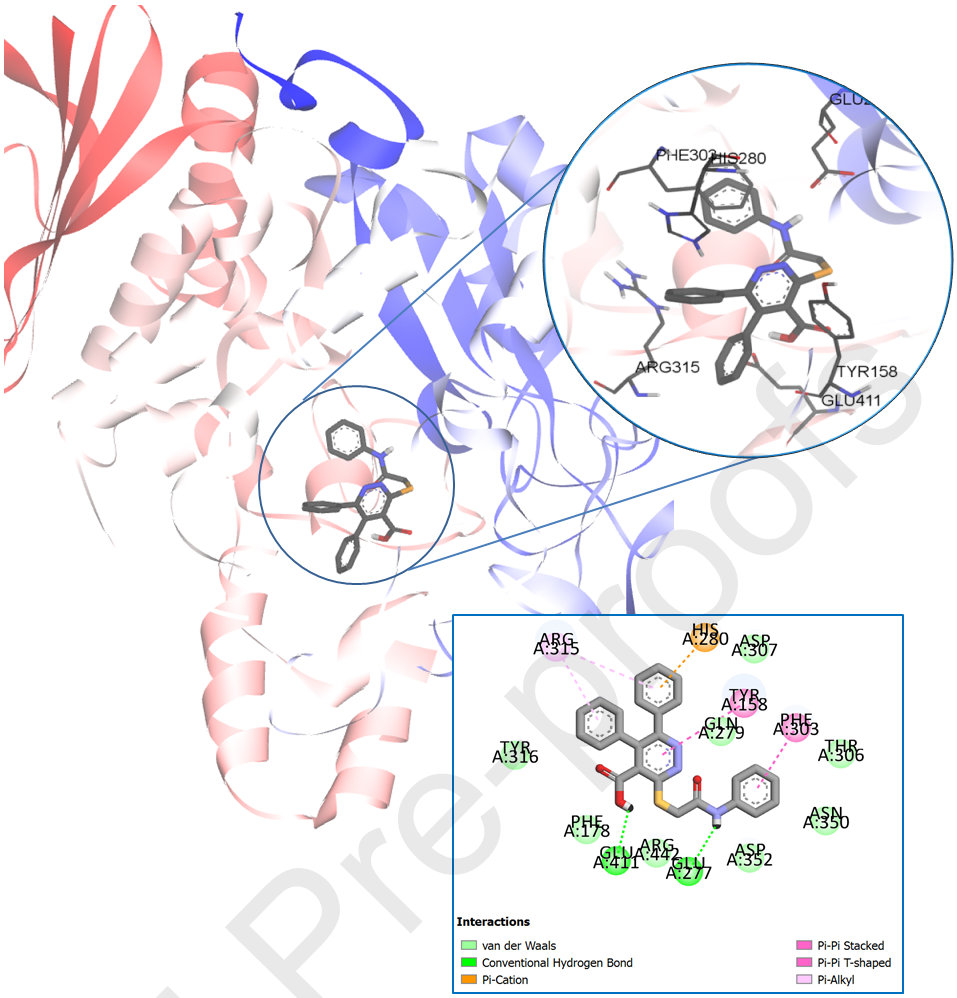

Figure 4. 3D binding conformation and 2D binding conformation of compound **8a.**

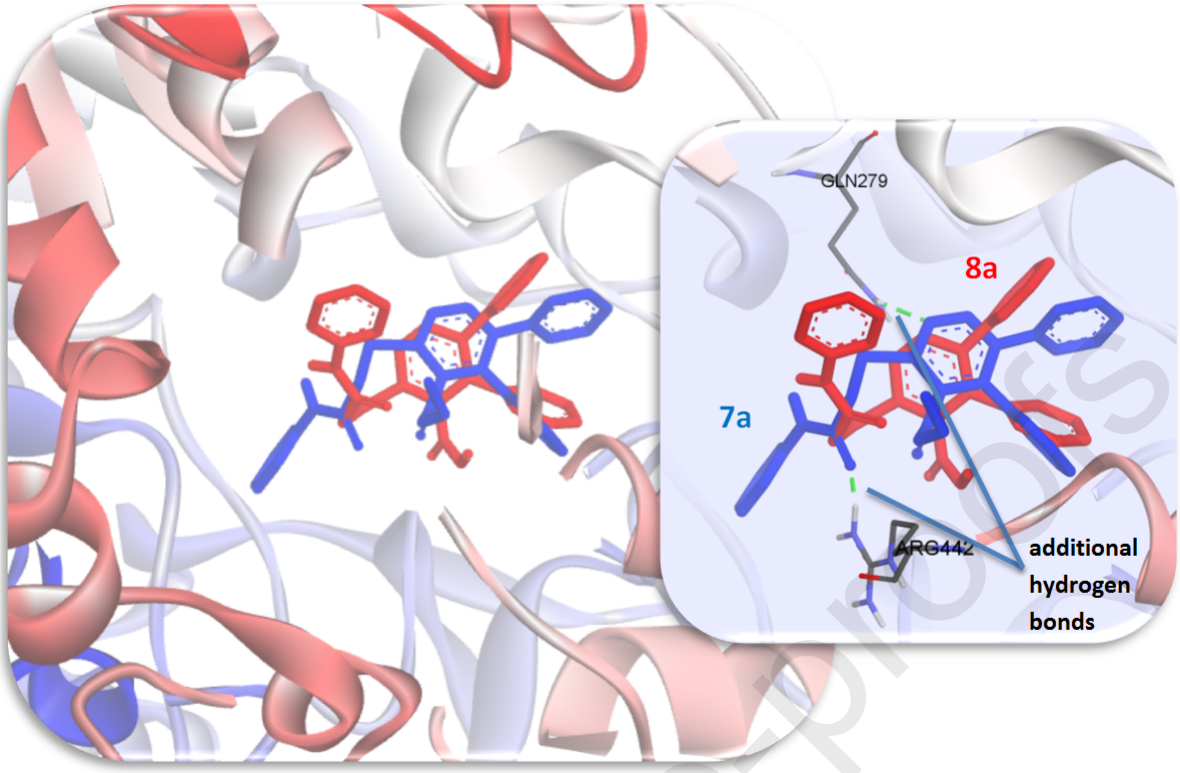

Figure 5. Molecular docking comparison of compound **7a** in blue color with compound **8a** in red color.

4. Conclusion

In summary, we described the activity and structural characterization data for two series of pyridizine based α-glucosidase inhibitors. We performed *in-vitro* evaluation, cytotoxic, kinetic, and molecular docking studies. The *in-vitro* evaluation revealed that compound **7a** is 10-times more active than positive control with no cytotoxicity against the normal cell line. The docking studies rationalized the improved activity of compound **7a** compared with **8a**. The results of this study introduced pyridazine as the attractive core to discover potent inhibitors of α-glucosidase enzyme.

References

[1] Reaven GM. Role of insulin resistance in human disease. Diabetes 1988;37:1595-1607. https://doi.org/10.2337/diab.37.12.

[2] Marín-Peñalver JJ, Martín-Timón I, Sevillano-Collantes C, Del Cañizo-Gómez FJ. Update on the treatment of type 2 diabetes mellitus. World J Diabetes. 2016;15:354-395. https://doi.org/10.4239/wjd.v7.i17.354.

[3] Jain S, Saraf S. Type 2 diabetes mellitus—Its global prevalence and therapeutic strategies. Type 2 diabetes mellitus—Its global prevalence and therapeutic strategies. Diabetes Metab Syndr. 2010;4:48-56. https://doi.org/10.1016/j.dsx.2008.04.011.

[4] Derosa G, Maffioli P. Thiazolidinediones plus metformin association on body weight in patients with type 2 diabetes. Diabetes Res Clin Pract. 2011;91:265-270. https://doi.org/10.1016/j.diabres.2010.08.001.

[5] Cicero AF, Tartagni E, Ertek S. Metformin and its clinical use: new insights for an old drug in clinical practice. Arch Med Sci. 2012;9:907-917. https://doi.org/10.5114/aoms.2012.31622.

[6] Derosa G, Maffioli P. Dipeptidyl peptidase-4 inhibitors: 3 years of experience. Diabetes Technol Ther. 2012;14:350-364. https://doi.org/10.1089/dia.2011.0204.

[7] Derosa G, Maffioli P. GLP-1 agonists exenatide and liraglutide: a review about their safety and efficacy. Curr Clin Pharmacol. 2012;7:214-228. https://doi.org/10.2174/157488412800958686.

[8] Joshi SR, Standl E, Tong N, Shah P, Kalra S, Rathod R. Therapeutic potential of α-glucosidase inhibitors in type 2 diabetes mellitus: An evidence-based review. Expert Opin Pharmacother. 2015;16:1959-1981. https://doi.org/10.1517/14656566.2015.1070827.

[9] Holman RR, Cull CA, Turner RC. A randomized double-blind trial of acarbose in type 2 diabetes shows improved glycemic control over 3 years. Diabetes Care. 1999;22:960–964. https://doi.org/10.2337/diacare.22.6.960.

[10] Lebovitz HE. α-Glucosidase inhibitors. Endocrinol Metab Clin North. 1997;26:539-551. 10.1016/s0889-8529(05)70266-8.

[11] Truscheit E, Frommer W, Junge B, Muller L, Schmidit DD, Wingender W. Chemistry and biochemistry of microbial alpha-glucosidase inhibitors. Angew Chem Int Ed Engl. 1981;20:744-761. https://doi.org/10.1002/anie.198107441.

[12] Bischoff H. Effect of acarbose on diabetic late complications and risk factors—New animal experimental results. Aktuel Endokrinol Stoffwechsel. 1991;12:25-32.

[13] Wehmeier UF, Piepersberg W. Biotechnology and molecular biology of the alpha-glucosidase inhibitor acarbose. Microbiol Biotechnol. 2004;63:613-625. https://doi.org/10.1007/s00253-003-1477-2.

[14] Bansal R, Thota S. Pyridazin-3(2H)-ones: the versatile pharmacophore of medicinal significance Med Chem Res. 2013;22:2539–2552. https://doi.org/10.1007/s00044-012-0261-1.

[15] Loksha YM, Abd-Alhasee MM. Synthesis and biological screening of some novel 6-substituted 2-alkylpyridazin-3(2H)-ones as anti-inflammatory and analgesic agents Arch Pharm Chem Life Sci. 2020;1900295. https://doi.org/10.1002/ardp.201900295.

[16] Singh B, Bhatia R, Pani B, Gupta D. Synthesis, crystal structures and biological evaluation of new pyridazine derivatives. J Mol Structure. 2020;1200:127084. https://doi.org/10.1016/j.molstruc.2019.127084.

[17] Harris RR, Black L, Surapaneni S, Kolasa T, Majest S, Namovic MT, Grayson G, Komater V, Wilcox D, King L, Marsh K, Jarvis MF, Nuss M, Nellans HL, Pruesser GA, Reinhart B, Cox P, Jacobson A, Stewart M, Carter CG, Bell RL. ABT-963 [2-(3, 4-difluoro-phenyl)-4-(3-hydroxy-3-methyl-butoxy)-5-(4-methanesulfonyl-phenyl)-2H-pyridazin-3-one], a highly potent and selective disubstituted pyridazinone cyclooxgenase-2 inhibitor. J Pharmacol Exp Ther. 2004;311:904-912. https://doi.org/10.1124/jpet.104.070052.

[18] Sharma D, Bansal R. Synthesis of 2-substituted-4-aryl-6-phenylpyridazin-3(2H)-ones as potential anti-inflammatory and analgesic agents with cardioprotective and ulcerogenic sparing effects. Med Chem Res. 2016;25:1574-1589. https://doi.org/10.1007/s00044-016-1588-9.

[19] Ahmed EM, Hassan MSA, El-Malah AA, Kassab AE. New pyridazine derivatives as selective COX-2 inhibitors and potential antiinflammatory agents; design, synthesis and biological evaluation. Bioorg Chem. 2020;95:103497. https://doi.org/10.1016/j.bioorg.2019.103497.

[20] Gosnell ES, Thikkurissy S. Assessment and Management of Pain in the Pediatric Patient. Pediatric Dentistry (Sixth Edition) Infancy Through Adolescence. 2019, Pages 97-115. https://doi.org/10.1016/B978-0-323-60826-8.00007-9.

[21] Lima LM, Barreiro EJ. Bioisosterism: a useful strategy for molecular modification and drug design. Curr Med Chem. 2005;12:23-49.https://doi.org/10.2174/0929867053363540.

[22] Patani GA, LaVoie EJ. Bioisosterism: A Rational Approach in Drug Design. Chem Rev. 1996;96:8, 3147-3176. https://doi.org/10.1021/cr950066q.

[23] Wang G, Li X, Wang J, Xie Z, Li L, Chen M, Chen S, Peng Y. Synthesis, molecular docking and a-glucosidase inhibition of 2-((5,6-diphenyl-1,2,4-triazin-3-yl)thio)-N-arylacetamides. Bioorg Med Chem Lett. 2017;27:1115-1118. http://dx.doi.org/10.1016/j.bmcl.2017.01.094.

[24] Wang G, Wang J, He D, Li X, Li J, Peng Z. Synthesis and biological evaluation of novel 1,2,4-triazine derivatives bearing carbazole moiety as potent α-glucosidase inhibitors Bioorg Med Chem Lett. 2016;26:2806-2809. https://doi.org/10.1016/j.bmcl.2016.04.071.

[25] Wang G, Peng Z, Wang J, Li X, Li J, Synthesis, in vitro evaluation and molecular docking studies of novel triazine-triazole derivatives as potential α-glucosidase inhibitors. Eur J Med Chem. 2017;125:423-429. https://doi.org/10.1016/j.ejmech.2016.09.067.

[26] Rahim F, Ullah K, Ullah H, Wadood A, Taha M, Ur Rehman A, Imad Uddin, Ashraf M, Shaukat A, Rehman W, Hussain S, Mohammed Khan K. Triazinoindole analogs as potent inhibitors of α-glucosidase: Synthesis, biological evaluation and molecular docking studies. Bioorg Chem. 2015;58:81-87. https://doi.org/10.1016/j.bioorg.2014.12.001.

[27] Wang G, Wang J, He D, Li X, Li J, Peng Z. One-Pot and Three-Component Synthesis, Characterization and Biological Evaluation of Some New 1,2,4-Triazine-coumarins. Heterocycles, 2016;92:1430-1439. https://doi.org/10.3987/COM-16-13491.

[28] Peytam F, Adib M, Shourgeshty R, Firoozpour L, Rahmanian-Jaz-M, Jahani M, Moghimi S, Divsalar K, Faramarzi MA, Mojtabavi S, Safari F, Mahdavi M, Foroumadi A. An efficient and targeted synthetic approach towards new highly substituted 6-amino-pyrazolo[1,5-a]pyrimidines with α-glucosidase inhibitory activity. Sci Rep. 2020;10:2595. https://doi.org/10.1038/s41598-020-59079-z.

[29] Toolabi M, Moghimi S, OghabiBakhshaiesh T, Salarinejad S, Aghcheli A, Hasanvand Z, Nazeri E, Khalaj A, Esmaeili R, Foroumadi A. 6-Cinnamoyl-4-arylaminothienopyrimidines as highly potent cytotoxic agents: Design, synthesis and structure-activity relationship studies. Eur J Med Chem. 2020;185:111786. https://doi.org/10.1016/j.ejmech.2019.111786.

[30] Mojallal-Tabatabaei Z, Foroumadi P, Toolabi M, Goli F, Moghimi S, Kaboudanian-Ardestani S, Foroumadi A. 2-(Bipiperidin-1-yl)-5-(nitroaryl)-1,3,4-thiadiazoles: Synthesis, evaluation of in vitro leishmanicidal activity, and mechanism of action. Bioorg Med Chem. 2019;:3682-3691. https://doi.org/10.1016/j.bmc.2019.07.009.

[31] Faraji L, Nadri H, Moradi A, Bukhari SNA, Pakseresht B., Moghadam FH, Moghimi S, Abdollahi M, Khoobi M, Foroumadi A. Aminoalkyl-substituted flavonoids: synthesis, cholinesterase inhibition, β-amyloid aggregation, and neuroprotective study. Med Chem Res. 2019;28:974-983. https://doi.org/10.1007/s00044-019-02350-4.

[32] Yasser MSA, Al-kahraman, Yasinzai M, Singh GS. Evaluation of some classical hydrazones of ketones and 1,2-diketones as antileishmanial, antibacterial and antifungal agents. Arch Pharm Res. 2012;35:1009-1013. https://doi.org/10.1007/s12272-012-0608-7.

[33] Schmidt P, Druey J. Heilmittelchemische Studien in der heterocyclischen Reihe. 5. Mitteilung. Pyridazine II. Eine neue Pyridazinsynthese. Helv Chim Acta. 1954;15:134-140. https://doi.org/10.1002/hlca.19540370116.

[34] Arianna G, Bettinelli I, Barlocco DA, Byoung-Mog K, Tae-Sook J, Kyung-Hyun C, Toma L. Mono- or Diphenylpyridazines Connected to N-(2,4-Difluorophenyl)-N‘-heptylurea as Acyl-CoA:Cholesterol Acyltransferase Inhibitors. J Med Chem. 2005;48:7708-7713. https://doi.org/10.1021/jm050703x.

[35] Khanaposhtani MM, Rezaei S, Khalifeh R, Imanparast S, Faramarzi MA, Bahadorikhalili S, Safavi M, Bandarian F, Esfahani EN, Mahdavi M, Larijani B. Design, synthesis, docking study, α-glucosidase inhibition, and cytotoxic activities of acridine linked to thioacetamides as novel agents in treatment of type 2 diabetes. Bioorg Chem. 2018;80:288-195. https://doi.org/10.1016/j.bioorg.2018.06.035

Declaration of interests

☒ The authors declare that they have no known competing financial interests or personal relationships that could have appeared to influence the work reported in this paper.

☐The authors declare the following financial interests/personal relationships which may be considered as potential competing interests:

Design and synthesis of novel pyridazine *N*-aryl acetamides: In-vitro evaluation of α-glucosidase inhibition, docking, and kinetic studies

Setareh Moghimi [a], Mahsa Toolabi [b], Somayeh Salarinejad [c], Loghman Firoozpour [a], Seyed Esmaeil Sadat Ebrahimi [c], Fatemeh Safari [d], Mohammad Ali Faramarzi [e], Alireza Foroumadi [a, c, **]

[a] *Drug Design and Development Research Center, The Institute of Pharmaceutical Sciences (TIPS), Tehran University of Medical Sciences, Tehran, Iran*

[b] *Department of Medicinal Chemistry, School of Pharmacy, Ahvaz Jundishapur University of Medical Sciences, Ahvaz, Iran*

[c] *Department of Medicinal Chemistry, Faculty of Pharmacy, Tehran University of Medical Sciences, Tehran, Iran*

[d] *Department of Biology, Faculty of Science, University of Guilan, Rasht, Iran*

[e] *Department of Pharmaceutical Biotechnology, Faculty of Pharmacy, Tehran University of Medical Sciences, Tehran, Iran*

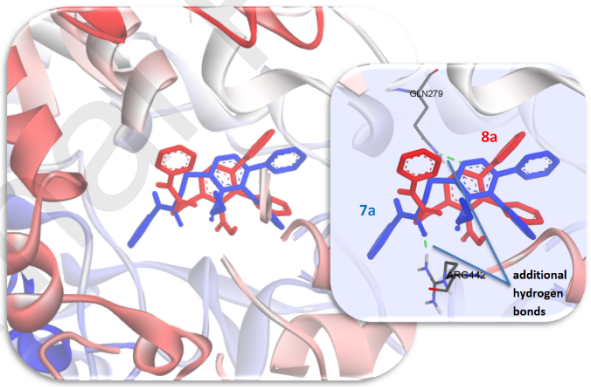

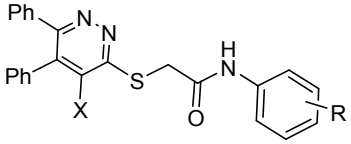

X = COOEt, COOH

R = H, Me, *i*-Pr, ethynyl, OMe, F, Cl, 3,5-*di*Cl, CN

Highlights

A new series of pyridazine-base compounds were synthesized as glucosidase inhibitor.

The most active compound was 10 times more active than acarbose.

Kinetic and molecular docking studies were performed to determine the mode of inhibition.